Novel Mobile Mechanism Design for an Obstacle-Overcoming Robot Using Rotating Spokes

YOUNGJOO LEE[1], **MYOUNGJAE SEO**[1], **SIJUN RYU**[1], **HWA SOO KIM**[2], **(Member, IEEE),**
AND TAEWON SEO[1], **(Senior Member, IEEE)**

[1]School of Mechanical Engineering, Hanyang University, Seoul 04763, South Korea
[2]School of Mechanical System Engineering, Kyonggi University, Suwon 16227, South Korea

Corresponding author: Taewon Seo (taewonseo@hanyang.ac.kr)

ABSTRACT In this paper, a mechanism for overcoming high obstacles is proposed to broaden the application range of the exterior wall cleaning robot. The proposed one-degree-of-freedom wheel mechanism can overcome high obstacles by the rotation of a wheel with two different spoke lengths. To implement the inclined tilted wheel (ITW), two design variables were studied - a spoke assembly angle and a wheel shaft assembly angle. At the critical assembly angles of $\varphi = 45°$ and $\theta = 135°$, the characteristics of the generated wheel trajectory does not invade the upper and lower space of the robot. From the trajectory, the space efficiency can be secured for thrust unit cleaning device. And the same contact characteristics can get with the existing wheel on the surface. To secure the orientation stability after overcoming a high obstacle, the reaction force analysis at each caster was performed. Through the analysis results, the orientation stability was secured without the distance compensation at the gantry during or after overcoming obstacles. To verify the obstacle-overcoming ability of the ITW, a 6m - high - test bench and a 0.3m - high - obstacles was manufactured. With a scenario defining an angular position of ITW, the ability of overcoming obstacle was confirmed in the test. In addition, the scenario was supplemented for stable overcoming to avoid a collision against obstacles through additional experiments.

INDEX TERMS Inclined trajectory wheel (ITW), building surface cleaning robot, overcoming obstacles, wheel trajectory, leg wheel.
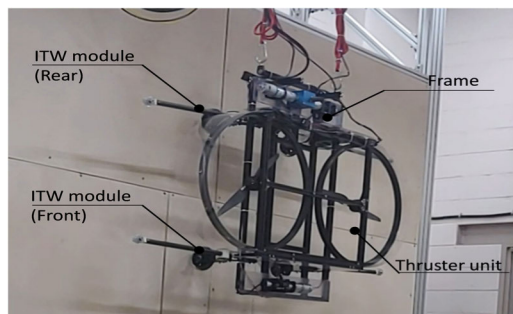
I. INTRODUCTION

Cleaning the exterior walls of buildings is an important task in terms of management annually. In particular, the demand for the maintenance of high-rise buildings is increasing. However, cleaning the exterior walls of high-rise buildings is an extremely dangerous, time-consuming task that has been performed utilizing the limited space such as the gondola. This has led to numerous workplace accidents every year.

Therefore, many researchers have been studied about the cleaning robot in order to replace humans in building exterior-wall cleaning sites [1]–[9]. The most well-known robots are TITO 500 [10], IPC EAGLE [11], SKYPRO [11],

The associate editor coordinating the review of this manuscript and approving it for publication was Aysegul Ucar.

SIRIUSc [12], and Sky Scraper -I [13] that move via ropes fixed with a winch system on the building tops. These robots have many advantages in terms of the simplicity of structure, installation, convenience of application, and cleaning performance. In particular, IPC EAGLE [11] and SKYPRO [11] have been commercialized and have even some line-ups. Robots attached to glass windows using strong vacuum adsorption pads, such as Gecko inspired robots [14]–[17] and Mantis [18], [19], have also been studied. In addition, robots using designated rails [20], [21] for building maintenance was developed.

The ability for overcoming obstacles is an essential for robots cleaning the exterior walls of buildings. So various obstacle overcoming mechanisms were applied. Robots using a large diameter brush, such as IPC EAGLE [11] and

FIGURE 1. Test robot with inclined trajectory wheels (ITWs) for overcoming obstacles on the wall surface.

SKYPRO [11] use a combination of wheels and a brush to achieve stable obstacle-overcoming ability. Robots using vacuum adsorption pads, such as those in Gecko inspired robots [14]–[17], and Mantis [18], [19] adopt mechanical link systems, or a mechanism utilizing the deformation of the adsorption plates to overcome obstacles. In addition, BWMR [20] and BFMR [21] used the designated rails installed at a height higher than the obstacle to avoid interference with the obstacle. Rope Rider [22] uses triangular track wheels for obstacles. Three-modular climbing-unit mechanism [23] and a tether compliance mechanism [13] were introduced to overcome obstacles.

However, previous cleaning robots have a low obstacle height. In case of the robot using brush for cleaning unit [11], [12], the overcoming height is determined by the brush size and wheels. So the applicability of these cleaning robots is restricted by the obstacle height. Another cleaning robot adopted the adsorption pad mechanism [14]–[19], [24], [25] have a low moving stroke for obstacles because of small displacement of the adsorption pad deformation. Therefore, it can be applied only to buildings with low obstacles, such as glass wall surfaces, and the applicability is substantially influenced by the details of grass wall frame.

Also space efficiency is lower in the view of robot layout, when a separate obstacle overcoming module is adopted. In the case of the existing commercialized cleaning robot, the obstacle overcoming module cannot be installed inside the robot due to the other unit. For example, Gecko inspired robots is required the vacuum unit in the body. Sky Scraper-I [13] needs a space for cleaning unit to move between the clamping arms. The three-modular obstacle-climbing robot [23] requires the module operating space inside the robot.

In this paper, we propose a wheel mechanism to overcome high obstacles, which designed with two design parameters, as shown in Fig. 1. The proposed mechanism is a one-degree-of-freedom (1-DOF) and uses an inclined trajectory. It is a simple principle for overcoming obstacles by using the difference in the length of the spokes while changing the positions of the two spokes. In addition, the overcoming height can be changed by exchanging the spoke length within the torque range and a max obstacle height.

TABLE 1. Design parameters of ITW and robot.

Parameters	Definition
φ	tilting angle between a driving shaft and a wheel axis
θ	assembly angle between a wheel base and a spoke
ϕ	angle between the rope and the wall surface
d	distance from the rope fastening position to mass center
β	angle when the two spokes touch on the wall

The proposed mechanism generating a specific trajectory provide space efficiency for other units. The trajectory generated by the spoke does not exceed the driving shaft height. Therefore, an interference with other devices installed in the upper and lower robot body space can be avoided. Also the generated trajectory has the same characteristics with conventional wheel contact against the surface. The proposed wheel does two roles: a running wheel and an obstacle overcome device. Therefore, a separate space is not required for an obstacle overcoming device. It increases the space efficiency and allows the robot to be manufactured in a compact manner.

In this study, the static analysis was conducted to find a moment balance condition and to secure the stable orientation of the robot after overcoming obstacle, which does not need to compensate the generated angle between rope and the wall surface. And the maximum torque was analyzed for an orientation analysis of the wheel and for a motor selection. To confirm the obstacle-overcoming ability of the proposed wheel, the robot with four inclined trajectory wheels (ITWs) was manufactured. In addition, a scenario which maps the angle displacement plan of the wheels using four steps was applied to overcome an obstacle. A test bench with a height of 6 m was built, and the proposed wheel mechanism was observed to overcome a 300-mm obstacle.

The remainder of this paper is organized as follows. Section 2 explains the proposed the wheel shape design and a mechanism analysis. Section 3 presents the test robot configuration applied to the proposed wheel. Section 4 presents the experimental test setup and results. Section 5 provides a summary of this study and future work.

II. INCLINED TRAJECTORY WHEEL MECHANISM
The cleaning robot is composed of winches, thrusters, frame, cleaning devices, and electronic devices, which are assembled in a limited space. Not only the obstacle-overcoming mechanism should overcome high obstacles, but also it should be a space-efficient structure. There should be no interference regardless of the size of other components, and each assembly has to operate in the designated space when overcoming high obstacles. In addition, more space is required for the cleaning device installed under the robot body. We introduce a mechanism that addresses the aforementioned issues in the following subsections

A. WHEEL DESIGN PARAMETERS AND TRAJECTORY ANALYSIS
The proposed mechanism is a one-degree-of-freedom system. The proposed system has three geometric design parameters,
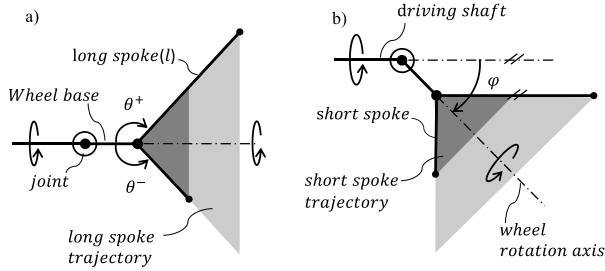
FIGURE 2. Proposed wheel concept and design parameters. The proposed wheel has two design parameters (θ, φ). a) θ is the assembly angle between the wheel base and the spoke. b) φ is a tilting angle between the driving shaft and the wheel rotation axis.

FIGURE 3. Inclined wheel trajectories at $\theta = 135°$, $\varphi = 45°$ in XY and YZ plane. Spoke length affects only the size of spoke trajectory. It shows the trajectory characteristics of the proposed wheel.

namely, two spokes assembly angles (θ, φ) and spoke length (l_L), as shown in Fig. 2 and Table 1. The angle θ is defined as the spoke assembly angle between the wheel base and the spoke, whereas the angle φ is defined as a tilting angle between the driving shaft and the wheel rotation axis. The pivoting center of the parameter φ is the universal joint that connects the wheel base and driving shaft, and l_L is the length of the long spoke.

The two angles (θ, φ) are parameters deciding various triangular cross-sectional shapes when the wheel rotates. From the geometrical characteristics of the proposed wheel, the sum of θ and φ have a critical angle relation. And a trajectory which is parallel with the driving shaft can be obtained. Then, the relation of two angles is given as the following condition:

$$\theta^+ + \varphi = 180° \qquad (1)$$

Here, θ^+ denotes the rotation of the clockwise direction. Under these conditions, the wheel trajectory which is a unique geometric feature that does not rise to the top of the robot can be made, as shown in Fig. 2 b). As the space can be clearly divided, the space efficiency can be improved in the robot layout.

The trajectory of a proposed wheel mechanism contact perpendicularly on the surface, similar with a typical wheel. When the spoke is rotated counterclockwise by θ and wheel rotation axis rotates counterclockwise by φ around the joint, the spoke trajectory becomes perpendicular to the wall at critical value as shown in Fig. 2. Therefore, the relation between θ and φ can be expressed as follows:

$$\theta^- - \varphi = 90° \qquad (2)$$

Here, θ^- denotes the counterclockwise rotation. The mechanism needs to examine the region of the wheel trajectory generated according to the range of φ. In the case of $0° < \varphi < 45°$ under the condition in Equation (1), the smaller the angle, the smaller are the obstacles overcoming height of generated trajectory by the geometrical relation. In the case of $45° < \varphi < 90°$, the trajectory creates the problems by the wheel shape. As the angle increases, the height to overcome obstacles also decreases. Moreover, as the trajectory invades the lower space of the robot, it may cause interference with the cleaning device. In the view of the posture
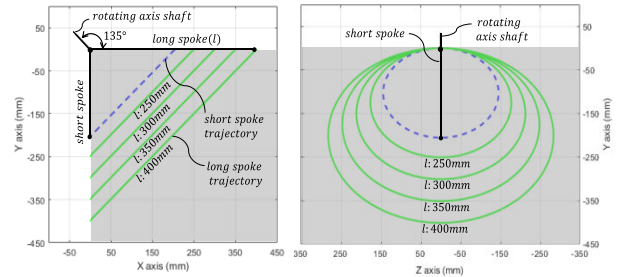
stability, because of the reduced support distance between wheels, the posture stability can be reduced when overcoming obstacles.

When $\varphi = 45°$ as a critical angle, many advantages are generated in the view of the performance and robot layout. The high obstacle can overcome with the generated spoke shape without reducing the robot's posture stability. In addition, the wheel spoke is not only perpendicular to the wall, but also parallel with wall. So the previously mentioned stable contact and the space efficiency can be secured. So the desired trajectory and wheel geometric shape can be obtained under two conditions (1) and (2). The wheel design angles are $\theta = 135°$ and $\varphi = 45°$.

The spoke length is a not a design parameter determining wheel trajectory characteristics. Because the spoke length is determined by other specifications and it determines only the ratio of the triangular cross section area of the trajectory as show in Fig. 3. The long spoke length is determined by the layout range of the robot body where the spokes between the front and rear wheels does not interfere with each other. And the short spoke length is determined by the cleaning device specification (such as spraying distance).

### B. OBSTACLE-OVERCOMING CONCEPT AND SCENARIO

The basic concept for obstacle-overcoming is using the rotation of the wheel assembled with different spoke lengths. The proposed mechanism proceeds sequentially in four steps: approach, lift-up, climbing, and landing, as shown in Fig. 4 and Fig. 5 a).
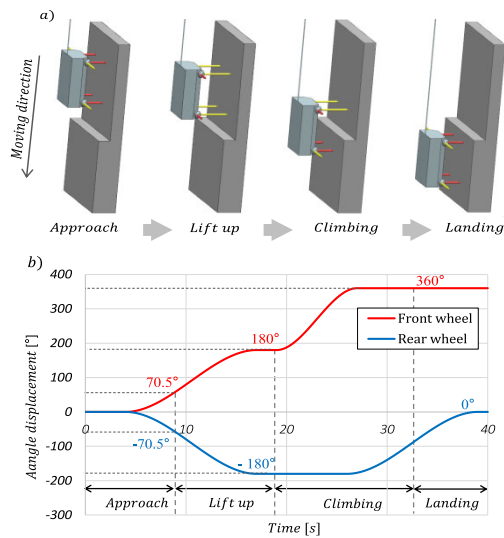
1) APPROACH

As the robot moves downward, the robot stops in front of a designated distance. Front wheels and rear wheels start to rotate in the opposite direction until $\pm 70.5°$, which two spokes contact the surface at the same time.

2) LIFT-UP

The front wheel and the rear wheel rotate until $\pm 180°$. Which the both spoke positions are completely exchanged each other. The robot body is lifted up toward the vertical direction of the surface by the wheel rotation. As shown in Fig. 5, the robot body height is higher than the obstacle.
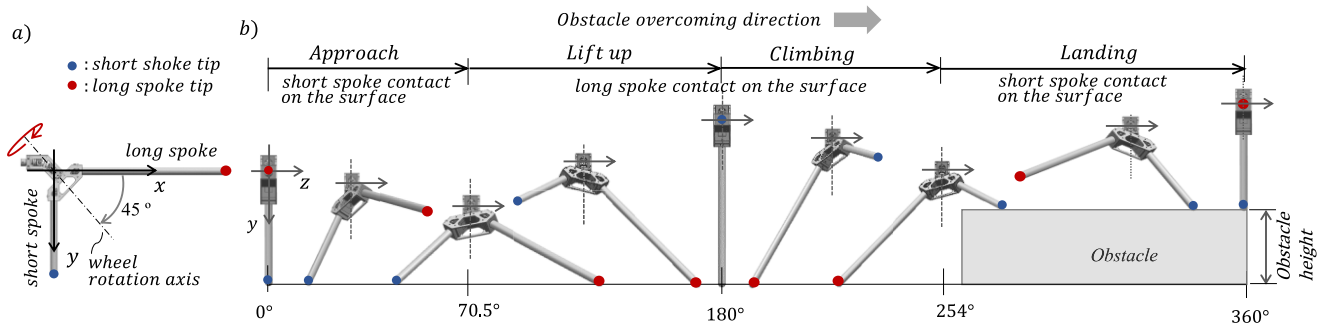
FIGURE 4. a) Concept design and b) the principle of the obstacle-overcoming of the inclined trajectory wheel. The proposed wheel comprises a spoke base and two different length spokes assembled at 45°. The principle of obstacle-overcoming is using the length-difference of two spokes. To distinguish the trajectory of the spokes, the ends of the short spokes were marked in blue circle, and the ends of the long spokes were marked in red circle.

FIGURE 5. Schematic diagram of obstacle-overcoming scenario. a) The scenario comprises four steps: *Approach, Lift-up, Climbing* and *Landing*. Red color is a short spoke; Yellow color is a long spoke. b) Angle position diagram of obstacle-overcoming scenario.

3) CLIMBING

As the front wheel rotates until 360°, the short spoke steps on top of the obstacle. So the robot can climb up by the wheel rotation. But the rear wheel does not rotate.

4) LANDING

The short spoke of a rear wheel lands on the upper surface of an obstacle. Until the short spoke return to the initial position (until - 0°), the rear wheel rotates, as shown in Fig. 5 b)

After overcoming the obstacle, an angle ϕ is generated between the rope and the wall. When it is larger than a critical angle, the robot becomes unstable. The stable condition, the angle and distance variables, is examined in next chapter.

C. STATIC ANALYSIS FOR THE STABILITY

When the short spokes of the front or rear wheels fell off the wall, the robot becomes unstable. This was caused by the moment imbalance of the robot. To secure the stability of the robot, the static analysis was performed. In order to compensate for the stability, the force and moment balance condition should be satisfied like Equation (4).

TABLE 2. Values of static analysis for proposed 1-dof wheel.

| Symbol	Value	Symbol	value
a	280 mm	m	10 kg
b	313 mm	ϕ	4°
c	33 mm	F_T	30 N
e	475 mm	l_L	420 mm
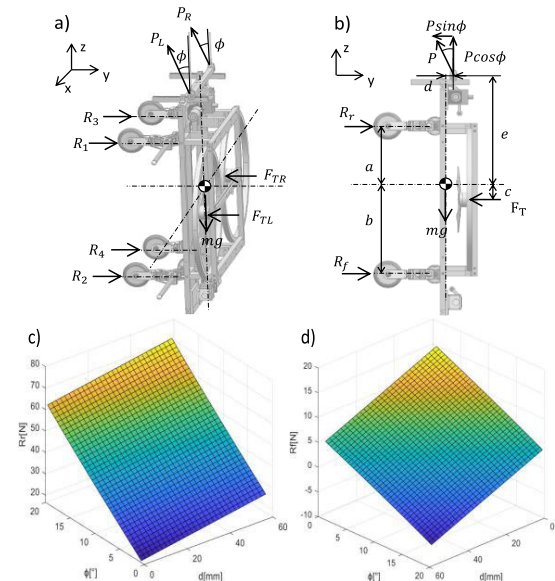
FIGURE 6. FBDs with a) forces and reaction forces in XYZ coordinator. b) Simplified FBD in YZ plane. From the symmetrical structure of the robot, forces (F_T, R, P) can be expressed single force. And the static analysis result of c) R_r d) R_f depending on variables ϕ and d.

The variables for the moment balance are a distance d and an angle ϕ. d is a distance between the mass center of the robot and the rope fastening position in y direction. And ϕ is an angle between the rope and the wall surface, which is created after the robot overcomes the obstacle. In particular, the angle becomes larger when shorter the distance, it affects the stability.

The free-body diagram (FBD) is shown in Fig. 6 a). Assuming that the robot is symmetric and the center of mass is on the Z axis. The rope tension P and thrust force F_T can be simplified as shown in Fig. 6 b). So the reaction force can be expressed as follows:

$$R_f = R_2 + R_4, \quad R_r = R_1 + R_3 \qquad (3)$$
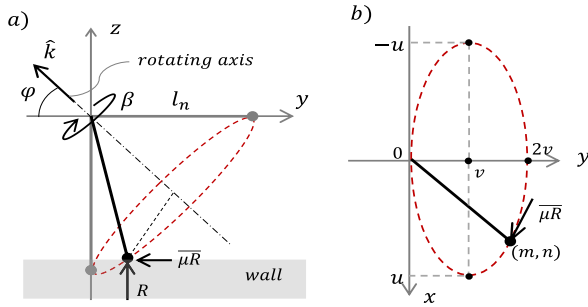
FIGURE 7. Scheme of FBDs for maximum torque calculation. (a) Diagram of FBD when a long spoke contact on the wall. (b) A projected trajectory (ellipse) on the x-y plane and friction force μR which is tangent on the projected trajectory.

Under the precondition of no-slip on the wall, the following equations is able to derived:

$$\begin{cases} \sum F_z = 0 : P c\phi - mg = 0 \\ \sum F_y = 0 : -P s\phi - F_T + R_r + R_{fr} = 0 \\ \sum M_x = 0 : a R_r - b R_f + F_T c - e P s\phi - d P c\phi = 0 \end{cases} \tag{4}$$

From the Equation (4), the wheel reaction force R_r and R_f, can be obtained as in Equation (5)

$$\begin{cases} R_r = \dfrac{[(b-c)F_T + ((b+e)\tan\phi + d)mg]}{a+b} \\ R_f = \dfrac{[(a+c)F_T + ((a-e)\tan\phi - d)mg]}{a+b} \end{cases} \tag{5}$$

Here, $a \sim e$ denotes the distance from the center of mass, and mg, F_T denotes the force acting on the robot shown in Table 2.

The analysis results of the reaction force by Equation (5) are shown in Fig. 6 c-d). From the result, the rear wheels are always in contact with the wall regardless of ϕ and d, because $R_r > 0$. However, in case of the front wheel, an unstable condition exits depend on the R_f range. When $R_f \leq 0$, it suggest a criterion for determining the robot's posture stability. In this region where R_f is negative, R_r increases rapidly. This is because R_f cannot sustain the reaction force, R_r should support all reaction force alone. This means that the caster of the front wheel does not touch the surface and the robot body rotates around the rear wheel. This can be seen from Fig. 6 d) that the larger the angle and the longer the length, the larger the negative R_f value. The theoretical maximum angle ϕ is 23.5°. But under the practical conditions, such as the vibration and inertia force by winch, the maximum angle is about 10°. In consideration of the robot layout and the relation between the obstacle height and distance from the gantry, the variables are determined as $d = 15$ mm and $\phi = 4°$. From the decided variable the proposed robot is designed to have a reaction force of $R_r = 25.7$ N and $R_f = 11.1$ N.

D. MAXIMUM TORQUE

The maximum torque required to overcome obstacles was analyzed through proposed wheel geometric characteristics. FBD is illustrated in the XY plane, as shown in Fig. 7. The
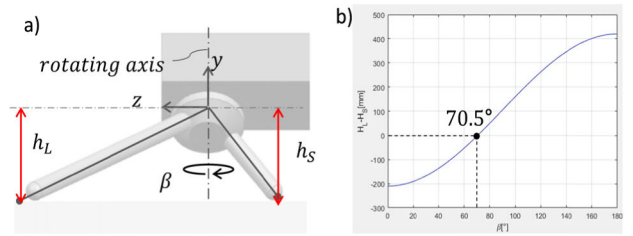
FIGURE 8. a) h_l, h_s are z coordinate of two spoke tips respectively. b) When $h_L - h_s = 0$, two spokes contact on the surface simultaneously at the angle of $\beta = 70.5°$.

torque required to overcome the obstacle can be obtained through Equation (6).

$$T = l \times F = (A_k * l_L \times F) . \hat{k} \tag{6}$$

$$A_k = e^{\hat{k}\beta} = I + \hat{k}s_\beta + \hat{k}^2 h_\beta$$

$$= \begin{bmatrix} k_1^2 h_\beta + c_\beta & k_1 k_2 h_\beta - k_3 s_\beta & k_1 k_3 h_\beta + k_2 s_\beta \\ k_1 k_2 h_\beta + k_3 s_\beta & k_2^2 h_\beta + c_\beta & k_2 k_3 h_\beta - k_1 s_\beta \\ k_1 k_3 h_\beta - k_2 s_\beta & k_2 k_3 h_\beta + k_1 s_\beta & k_3^2 h_\beta + c_\beta \end{bmatrix} \tag{7}$$

Here, A_k is the rotation matrix rotating about $\hat{k}$; β is rotational angle. $h_\beta = 1 - c\beta$, and s_β, c_β are the symbols for $sin\beta$, $cos\beta$, respectively. Further, I is the identity matrix, l_L is the long spoke matrix, $\hat{k}$ is a vector in the rotational axis. F consist of the reaction force calculated from Equation (5) and the friction force which is tangential direction of the projected spoke trajectory as shown in Fig 7 b).

$$\hat{k} = \begin{bmatrix} k_1 \\ k_2 \\ k_3 \end{bmatrix} = \begin{bmatrix} 0 \\ -cos\varphi \\ sin\varphi \end{bmatrix}, \quad l_L = \begin{bmatrix} 0 \\ l_L \\ 0 \end{bmatrix} \tag{8}$$

$$F = \begin{bmatrix} \mu R_x \\ \mu R_y \\ R \end{bmatrix} \tag{9}$$

μ is friction coefficient. μR_x and μR_y are the friction force element of μR. It can be get from Equation (10) which is projected wheel trajectory and Equation (11) which is a tangential vector on the projected wheel trajectory at the angle β.

$$\frac{x^2}{u^2} + \frac{(y-v)^2}{v^2} = 1 \tag{10}$$

$$\overline{\mu R} = \frac{\mu R}{\sqrt{(nv^2)^2 + (u^2(y-v))^2}} \left(nv^2 \hat{x} + u^2 (v-m) \hat{y} \right) \tag{11}$$

Here $u = l_L$, $v = 0.5 l_L$. And (m, n) is the coordinate of long spoke tip at angle β on Equation (10).

The angle β should be determined for the maximum torque. It can be obtained from the geometric characteristics of the proposed wheel, as shown in Fig. 8 a). When the small spokes fall off the wall after the two spokes touch the wall, the maximum torque is required. When the height between the two spoke tips ($h_L = h_s$) are the same,
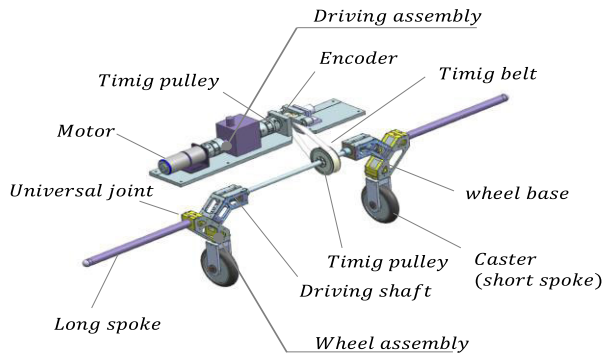
FIGURE 9. Configuration of the ITW module.

β can be obtained as:

$$-A_{\hat{k}}(\beta) \, l_L \big|_z - A_{\hat{k}}(\beta) \, l_S \big|_z = 0 \quad (12)$$

$$l_S = \begin{bmatrix} 0 \\ 0 \\ -l_S \end{bmatrix} \quad (13)$$

Here, l_S is the short spoke matrix. From the result is shown in Fig. 8 b). β is about 70.5°. /

The maximum height of the obstacles that the proposed wheel can overcome is determined by the height that a small spork is placed on top of the obstacle. It can be analyzed through the Equation (12). If $h_L - h_s$ is larger than an obstacle height, the wheel can overcome the obstacle. In case of the wheel specification designed in this study, the maximum height that a small spoke step on top of an obstacle without any interference with cast frame is 339mm at $\beta = 222°$. Considering the thickness of the caster, the maximum height of overcoming obstacles is about 330mm.

III. ROBOT CONFIGURATION WITH ITW

The robot with an ITW mechanism for overcoming obstacles comprises four parts: a frame, two ITW modules, a thrust unit, and electronics as shown in Fig. 1 and Fig 9. The robot size is 1290 mm (width) $\times$ 960 mm (height) $\times$ 410 mm (depth). The ITW module is assembled at the front and rear sides of the robot frame.

A. ITW AND ITW MODULE

The proposed ITW module comprises a wheel assembly and a driving assembly as shown in Fig. 9). The wheel assembly consist of two ITW units, a driving shaft and a small timing pulley, and joint units. And driving assembly consist of a driving motor, a timing pulley, a power transmission shaft, and sensors (an encoder and a torque sensor). The driving assembly is assembled at the upper space of the frame and the wheel assembly is assembled at the under. By using timing belt, the torque is transferred from the driving assembly to the wheel assembly.

ITW consists of two spokes, a wheelbase, a universal joint and its housing. A caster is adopted instead of the short spoke for low height obstacle. Two spokes are assembled at 90° phase on the wheel base. The double universal joint is
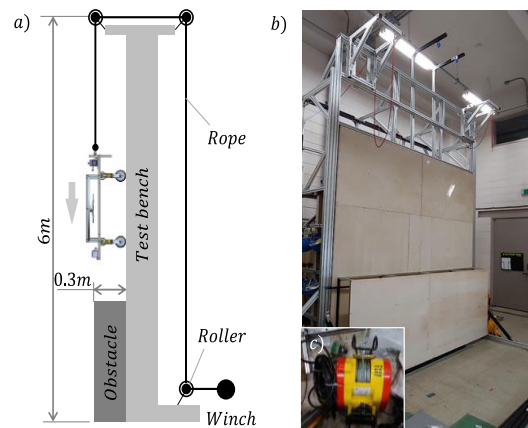

FIGURE 10. Experimental test bench. (a) Test bench configuration. (b) the created the test bench (c) winch.

TABLE 3. Specifications of robot comments.

| Component	Specifications
Driving motor	Geared motor, PG42-3657-12180, 1/104
Thruster size	18 × 6.1, carbon (T-motor)
Thruster motor	U7 series V2.0 BL(T-motor)
Torque sensor	BRDM-50
Proximity sensor	UDS10A/W328
Encoder	E30S4 Series, Autonics
Pulley reduction ratio	1:3, 2GT timing belt & pulley
Spoke	Carbon pipe, Diameter: 25mm
Universal joint	Double universal joint type, HJD 14

adopted to transfer the torque transition path is tilted by the angle φ. The joints can transmit a high torque without slip, also it is not sensitive to assembly tolerances. A timing belt and pulleys were used for the precise angle position and for reliable torque transmission. To secure motor torque of ITW, a 1:3 pulley reduction ratio was adopted. The applied geared motor has 4 Nm related torque at 170 rpm.

B. FRAME AND THRUSTER UNIT

For a high structural strength and a light weight, an industrial aluminum profile was applied. For the easy distance control as a translational joint (for variable d), the profile groove is used. For the free rotation at the rope knot, bearing is used. To attach the robot to the building surface, two thrusters were applied, as shown in Fig. 9. The large space for the thrust unit is secured from the geometrical characteristics of the ITW trajectory without any interference. The propeller driving motors are the U7 series, which is lightweight and has a wide speed control range. For the stable thrust force, voltage of 24V was supplied with additional power source.

C. CONTROL AND SENSORS

The ITW robot uses the pulse-width modulation (PWM) control for the wheel rotation. To measure the angle and check the distance from the surface, the sensors were applied as shown in Fig. 9. Two encoders were applied to measure the rotation of the front and rear wheels. A torque sensor was applied to monitor the torque required by the robot during the lift-up process. Two proximity sensors were applied to detect an obstacle and to provide a trigger signal at a designated
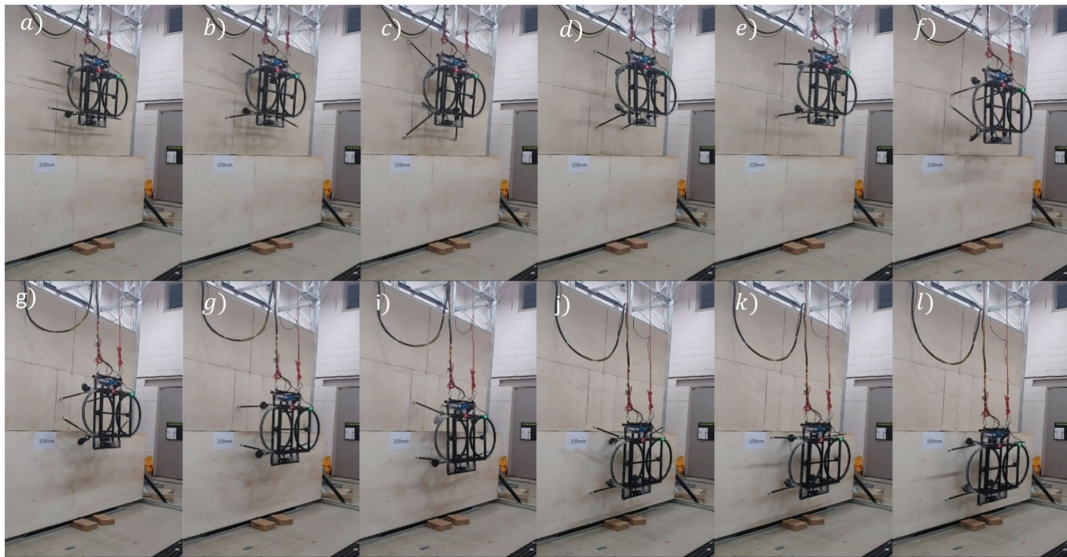
FIGURE 11. Test results of obstacle overcoming at height of 300 mm. The overcoming-obstacle process has 4 steps. These are the (a-c) Approach, (d–f) Lift-up, (g–k) Climbing, and (j) Landing.

distance to begin the obstacle overcoming process. The wheel position control is conducted through Proportional Integral Differential (PID) control through angular position feedback. Since the thruster rotates at a high speed, a separate control device and power supply were used during the experiments for the thruster unit.

IV. EXPERIMENT SETUP AND TEST RESULTS

A. TEST BENCH SETUP AND THRUST FORCE

To verify the obstacle-overcoming ability of the proposed mechanism, a test bench was created, as shown in Fig. 10. The test bench comprises three parts: the mainframe, an obstacle, and a winch.

The height of the main frame is 6 m. In the main frame, rollers were placed at the top and rear side and a winch is installed at the bottom. The winch can lift up or down the 100-kg weight at a constant speed of 5 m/min. The target obstacle height was determined to be 300 mm, based on the results of Reference [1]. So when the robot has an ability to overcome a 300mm-height-obstacles, the robots can be applied to most buildings. The direction of overcoming the obstacle is downward, as shown in Fig. 10. It has advantages in terms of system configuration and system control. Also the recontamination can be avoided and the classification of the cleaned area becomes easier. Based on these advantages, the commercialized cleaning robots move downward from the top of the building. Through the thrust force measuring the experiment, it was confirmed that 15N of thrust force was generated at approximately 4250 rpm. So 30N can be generated with two thrusters. The speed deviation of the two thrusters is less than 2%.

B. TEST RESULTS AND THE DISCUSSION

Through the experimental test, the characteristics of the proposed mechanism and the ability to overcome obstacles were verified. The robot adopted the ITW module could overcome
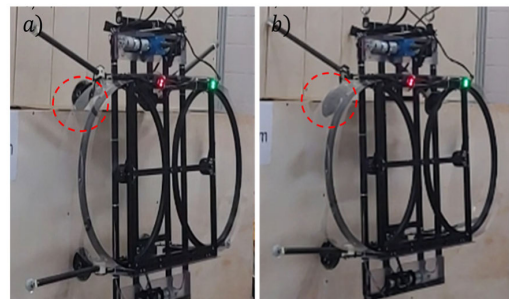

FIGURE 12. a) Rear wheel caster interference with the obstacles. b) Improved lending approach.

a 300 mm-high obstacle using the scenario shown in Fig. 5. Also it is confirmed that the wheel trajectory does not interfere with the thrust unit space and the under space of the robot in the process of overcoming obstacles.

The orientation stability was verified after overcoming high obstacles without the distance compensation between the rope and wall as much as the height of the obstacle. Also the body balancing moment was well balanced and four casters contacted on the wall stably under the condition of $d = 15mm$, $\phi = 4°$, even with a small thrust force. The measured maximum torque in the test was 5.4 Nm. But this value is different with the theoretical maximum torque, which is approximately 4.9 Nm at $\beta = 70.5°$ through Equation (10). The difference between the calculated and the measured is occurred by an unexpected friction. Unexpected friction occurred because the rotation direction of small cast applied for smooth movement at the long spoke tips did not match the direction of the spoke trajectory.

In the landing step, the collided between the obstacle edgy and the rear wheel cast was identified, as shown in Fig.12 a). It is an important issue, because it can damage the building surface. The reason of collision is the narrowed space as the large thrust force pushes the robot to the wall during
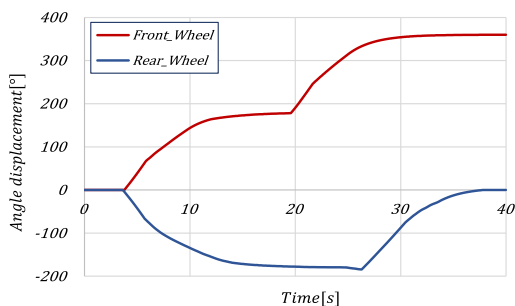
FIGURE 13. Measured angle position dates by the encoders, which is modified to avoid bumped with obstacles.

the climbing process. The first approach for this issue is to secure the space by reducing the thrust force. But it is not a fundamental solution when robot's body vibrates backward and forward. The second approach is to use the geometric properties of the ITW mechanism. As the rear wheel rotates slowly until passing through an obstacle edges and then returns late to its initial position by time sequence, as shown in Fig. 12b). So the collision can be avoided regardless of the space. So the effectiveness of the second approach were confirmed through the additional experiments. The modified scenario was confirmed that a collision can be avoided. The angle position profile of the modified scenario was measured by the encoder as shown in Figure 13.

V. CONCLUSION

A 1-DOF mechanism was proposed for a wall cleaning robot to overcome high obstacles. With two design parameters, inclined trajectory wheel (ITW) can be created at the angle of $\theta = 135°$, $\varphi = 45°$. The wheel uses the difference of two spoke length for obstacle overcoming. Based on the wheel design results, ITW robot was manufactured. The ability of the proposed mechanism was verified through a 300 mm-obstacle confirmed through the theoretical analysis and actual experiments, which does not invade to upper and lower space.

In the view of space-efficiency, the proposed wheel has an advantage on the cleaning robot layout to secure the space for other units. From the results of the reaction force analysis, $d = 15$ mm and $\phi = 4°$, the robot can to overcome high obstacles stably without distance compensation between rope and the wall.

In the near future, we will study the robot orientation stability under the condition of water jet spray while overcoming obstacles. And an active balancing control mechanism based on the closed loop output feedback control method [26] will be studied for the robot orientation stability simultaneously.

REFERENCES

[1] T. Seo, Y. Jeon, C. Park, and J. Kim, "Survey on glass and façade-cleaning robots: Climbing mechanisms, cleaning methods, and applications," *Int. J. Precis. Eng. Manuf.-Green Technol.*, vol. 6, no. 2, pp. 367–376, Apr. 2019.

[2] M. H. Korayem and H. Ghariblu, "Maximum allowable load on wheeled mobile manipulators imposing redundancy constraints," *Robot. Auton. Syst.*, vol. 44, no. 2, pp. 151–159, Aug. 2003.

[3] N. Mir-Nasiria, H. Siswoyo, and M. H. Ali, "Portable autonomous window cleaning robot," in *Proc. Int. Conf. Robot. Smart Manuf.*, 2018, pp. 197–204.

[4] J. Hong, S. Yoo, I. Joo, J. Kim, H. S. Kim, and T. Seo, "Optimal parameter design of a cleaning device for vertical glass surfaces," *Int. J. Precis. Eng. Manuf.*, vol. 20, no. 2, pp. 233–241, 2019.

[5] M. H. Korayem, H. Rahimi, and A. Nikoobin, "Path planning of mobile elastic robotic arms by indirect approach of optimal control," *J. Adv. Robot. Syst.*, vol. 8, no. 1, pp. 10–20, 2011.

[6] M. H. Korayem and S. Rafee, "The SDRE control of mobile base cooperative manipulators: Collision free path planning and moving obstacle avoidance," *Robot. Auton. Syst.*, vol. 86, pp. 86–105, Dec. 2016.

[7] S. Yoo, I. Joo, J. Hong, C. Park, J. Kim, H. S. Kim, and T. Seo, "Unmanned high-rise façade cleaning robot implemented on a gondola: Field test on 000-building in Korea," *IEEE Access*, vol. 7, pp. 30174–30184, 2019.

[8] S. Rajesh, P. Janarthanan, G. Raj, and A. Jaichandran, "Design and optimization of high rise building cleaner," *Int. J. Appl. Eng. Res.*, vol. 13, no. 9, pp. 6881–6885, 2018.

[9] Y.-H. Choi and K.-M. Jung, "Windoro: The world's first commercialized window cleaning robot for domestic use," in *Proc. 8th Int. Conf. Ubiquitous Robots Ambient Intell. (URAI)*, Nov. 2011, pp. 131–136.

[10] T. Akinfiev, M. Armada, and S. Nabulsi, "Climbing cleaning robot for vertical surfaces," *Ind. Robot, Int. J.*, vol. 36, no. 4, pp. 352–357, Jun. 2009.

[11] H. Fawzy, H. El Sherif, and A. Khamis, "Robotic façade cleaning system for high-rise building," in *Proc. 14th Int. Conf. Comput. Eng. Syst. (ICCES)*, Cairo, Egypt, Dec. 2019, pp. 282–287.

[12] N. Elkmann, T. Felsch, M. Sack, J. Saenz, and J. Hortig, "Innovative service robot systems for façade cleaning of difficult-to-access areas," in *Proc. IEEE/RSJ Int. Conf. Intell. Robots Syst.*, Lausanne, Switzerland, vol. 1, Sep./Oct. 2002, pp. 756–762.

[13] N. Imaoka, S.-G. Roh, N. Yusuke, and S. Hirose, "SkyScraper-I: Tethered whole windows cleaning robot," in *Proc. IEEE/RSJ Int. Conf. Intell. Robots Syst.*, Oct. 2010, pp. 5460–5465.

[14] C. Menon, M. Murphy, and M. Sitti, "Gecko inspired surface climbing robots," in *Proc. IEEE Int. Conf. Robot. Biomimetics*, Shenyang, China, Aug. 2004, pp. 431–436.

[15] F. Cepolina, R. Michelini, R. Razzoli, and M. Zoppi, "Gecko, a climbing robot for wall cleaning," in *Proc. 1st Int. Workshop Adv. Service Robot. (ASER)*, Bardolino, Italia, 2003, pp. 1–5.

[16] R. Chen, L. Fun, Y. Qiu, R. Song, and Y. Jin, "A gecko inspired wall-climbing robot based on vibration suction mechanism," *Proc. IMechE C*, vol. 233, nos. 19–20, pp. 7132–7143, Aug. 2019.

[17] F. García-Cárdenas, E. Escandón, and R. Canahuire, "Task space kinematic control of a gecko-inspired climbing robot with active suction cups," in *Proc. IEEE 26th Int. Conf. Electron., Electr. Eng. Comput. (INTERCON)*, Lima, Peru, Aug. 2019, pp. 1–4.

[18] M. Vega-Heredia, I. Muhammad, S. Ghanta, V. Ayyalusami, S. Aisyah, and M. R. Elara, "Multi-sensor orientation tracking for a façade-cleaning robot," *Sensors*, vol. 20, no. 5, p. 1483, Mar. 2020.

[19] M. Kouzehgar, Y. Tamilselvam, M. Heredia, and M. Elara, "Self-reconfigurable façade-cleaning robot equipped with deep-learning-based crack detection based on convolutional neural networks," *Autom. Construct.*, vol. 108, Dec. 2019, Art. no. 102959.

[20] S.-M. Moon, D. Hong, S.-W. Kim, and S. Park, "Building wall maintenance robot based on built-in guide rail," in *Proc. IEEE Int. Conf. Ind. Technol. (ICIT)*, Mar. 2012, pp. 498–503.

[21] S.-M. Moon, J. Huh, D. Hong, S. Lee, and C.-S. Han, "Vertical motion control of building façade maintenance robot with built-in guide rail," *Robot. Comput.-Integr. Manuf.*, vol. 31, pp. 11–20, Feb. 2015.

[22] K. Seo, S. Cho, T. Kim, J. Kim, and H. S. Kim, "Design and stability analysis of a novel wall-climbing robotic platform (ROPE RIDE)," *Mechanism Mach. Theory*, vol. 70, pp. 189–208, Dec. 2013.

[23] C. Lee and B. Chu, "Three-modular obstacle-climbing robot for cleaning windows on building exterior walls," *Int. J. Precis. Eng. Manuf.*, vol. 20, pp. 1371–1380, Aug. 2019.

[24] H. Zhang, J. Zhang, G. Zong, W. Wang, and R. Liu, "Sky cleaner 3: A real pneumatic climbing robot for glass-wall cleaning," *IEEE Robot. Autom. Mag.*, vol. 13, no. 1, pp. 32–41, Mar. 2006.

[25] M. Vega-Heredia, R. E. Mohan, T. Y. Wen, J. S. Aisyah, A. Vengadesh, S. Ghanta, and S. Vinu, "Design and modelling of a modular window cleaning robot," *Autom. Construct.*, vol. 103, pp. 268–278, Jul. 2019.

[26] H. Chen and N. Sun, "An output feedback approach for regulation of 5-DOF offshore cranes with ship yaw and roll perturbations," *IEEE Trans. Ind. Electron.*, early access, Feb. 2, 2021, doi: 10.1109/TIE.2021.3055159.

●●●